ICAS 2021 SHANG HAI
International Council of the Aeronautical Sciences
32nd Congress of the International Council of the Aeronautical Sciences
September 6-10, 2021
Pudong Shangri-La, Shanghai, China

Numerical simulation of sweeping motion effects on the hovering dragonflies

Zhichao Zhu [1], Bifeng Song [1], Wenqing Yang [1], Xinyu Lang [1]

[1]School of Aeronautics, Northwestern Polytechnical University, Xi'an, 710072, P. R. China
Phone: +0086 13752189768 Fax: +0086 029 88493278 Email:zhuzc980407@163.com

Abstract

In this paper, the typical hovering mode of dragonflies with different sweeping motions is numerically simulated by solving three-dimensional unsteady Navier-Stokes equations to explore the effects of stroke deviation on aerodynamic performance. A bionic wing model of dragonflies is applied, conducting a rotating motion around the parallel wing root axis-flapping, a rotating motion around the vertical axis-sweeping, and a rotating motion around 1/4 chord-pitching. Different parameters relevant to the aerodynamics of three-dimensional flapping tandem-wing have been studied, notably the sweeping amplitude. The results of this research show that for the hovering dragonflies, the sweeping motion increases the vertical force slightly, but the power consumption increases severely compared with the vertical force. The sweeping motion delays the shedding of trailing edge vortices during the stroke reversal. The leading edge vortices gradually increase in radius and fall off from the heel to the tip. Our research can provide reference for the design of dragonfly-like aircraft with multi degree of freedom motion.

Keywords: Hovering dragonflies; Numerical simulation; Sweeping amplitude

1. Introduction

In recent years, flapping-wing micro aerial vehicles (FMAVs) have attracted a lot of attention. Dragonflies are among the most agile flying insects. Dragonflies have attracted wide attention for their excellent hovering and fast forward flying ability.

Dickinson and Gotz et al.[1] found one of the key reasons for flapping wing in generating lift is the delayed stall by the LEV. Wakeling and Ellington[2] collected the kinematic parameters of dragonfly using a high-speed camera during its free-flying condition. It showed that the flapping of two wings is not completely in the vertical plane, but there is a certain angle between the flapping plane and the horizontal plane. Sane[3] discovered the LEV generates a low pressure region, which leads to an increase in suction on the wing surface. Thomas et al.[4] found that the flapping process of dragonflies utilized unsteady high lift mechanisms in typical low Reynolds number conditions, such as leading-edge vortex and wake capture, and the interaction between forewings and hindwings is the main form of unsteady high lift mechanisms Tsyuyki et al.[5] and Wakeling et al.[2] observed the flapping frequency of dragonflies wings and the results were 36Hz and 44Hz. Broering et al.[6] numerically investigated forward flight of the tandem wing in the case of in phase flutter, the tandem configuration produces larger thrust at high propulsion efficiency at the expense of lift efficiency. Chen et al.[7] observed the kinematic paramaters of the tethered dragonflies and found that the hindwings had asymmetric flapping obviously. Kok et al.[8] found that asymmetric motion can significantly improve lift and aerodynamic efficiency. Bomphrey et al.[9] measured the spanwise efficiency of six species of dragonflies in free flight, and found the correlation between spanwise efficiency and wing taper, indicating that the plane shape has an impact on the aerodynamic performance of insects. Li and Dong[10] focused on the wing kinematics of the dragonfly's turning process and found that the turning process is caused by the asymmetrical flapping of the wings on both sides. Luo et al.[11] explained

the influence mechanism of the stroke deviation: the added- rotation effect and the effective angle of attack of the wings. Hefler C et al.[12] found that the dragonflies' flight process uses the wake capture mechanism and the LEV delay stall mechanism. The LEV-LEV mutual interference process of the LEV of the forewings and the LEV of the hindwings. This LEV-LEV mutual interference can enhance the LEV volume of the hindwings and greatly increase the lift. Shanmugam et al.[13] used the CFD numerical simulation method to study the influence of the forewings and hindwings distance and phase difference of the two-dimensional tandem wing model, and found that the aerodynamic interference effect of the tandem wing strongly depends on the front and back distance and phase difference. Zou et al.[14] measured the flapping kinematics of dragonflies and found three-degree-of-freedom motions which are flapping, pitching, and sweeping motion during the hovering state. Nagai et al.[15] explored the effect of phase difference on the aerodynamic performance of tandem wings by experimental methods. Lehmann et al.[16] showed that under the typical phase difference of dragonfly, forewings and hindwings with similar length and aspect ratio could achieve the best lift coupling result, and the inconsistent length of forewings and hindwings would damage the lift of the coupling effect. Arranz et al.[17] used high-fidelity direct numerical simulation methods to study the aerodynamic performance of tandem wings with different aspect ratios. The fine flow field structure showed that the distance between forewings and hindwings would affect the shape of the vortex structure captured by the hindwings from the forewings.

At present, most of the researches focus on the aerodynamic interference mechanism between the forewings and hindwings in a certain flapping motion, such as flapping motion. The aerodynamic mechanism of multi degree of freedom motions of forewings and hindwings in tandem configuration, such as flapping and pitching motions, has not been revealed yet. The influence of the coordination of each movement is not clear. In order to understand the relationship between sweeping motion and other motions of flapping wing with tandem configuration, the typical hovering mode of dragonflies with different sweeping motions is numerically simulated by solving three-dimensional unsteady Navier-Stokes equations to explore the effects of stroke deviation on aerodynamic performance. Our research can provide reference for the multi-degree of freedom motion coupling of dragonfly-like aircraft.

2. Methods

2.1 Modelling and parameters

A bionic wing model of dragonflies which is obtained from the real dragonfly wings is applied, consisting of forewing (FW) and hindwing (HW). The shape of the wings is selected based on the biological data of the hovering dragonflies. Detailed geometry data is provided in Table 1. It moves around a plane, referred to as the stroke plane. Assuming the wings to be rigid, the bionic wing conducts a rotating motion around the parallel wing root axis-flapping, a rotating motion around the vertical axis-sweeping, and a rotating motion around 1/4 chord-pitching. The flapping kinematics are presented in Fig 1.

Table 1 - Geometry data

Paramaters	Value
Mean chord length of forewings (c_f)	8.67mm
Mean chord length of hindwings (c_h)	11.5mm
Semi-span of forewings (b_f)	47mm
Semi-span of hindwings (b_h)	45mm
Distance between forewings and hindwings (l/c_f)	0.9
Thickness (t/c)	0.02

Distance between the wing heel and the symmetry plane (R/c_f)	1

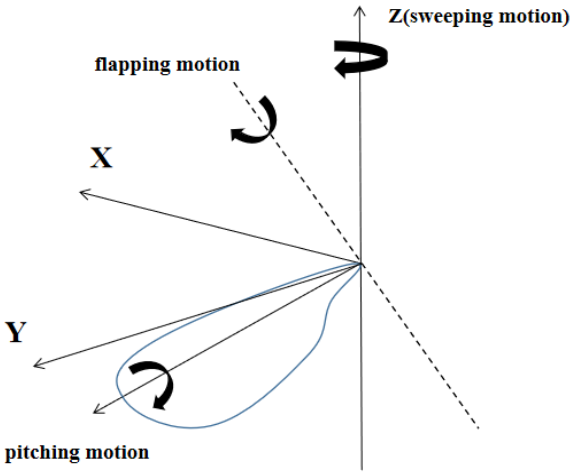

Fig 1 Definition of flapping, pitching and sweeping motion

The flapping motion of the FW and HW is represented as a simple sinusoidal function given by

$$\varphi(t) = \varphi_m \sin(2\pi ft) \quad (1)$$

The pitching motion of the FW and HW is represented as a simple sinusoidal function given by

$$\alpha(t) = \alpha_m \sin(2\pi ft - \pi) \quad (2)$$

The sweeping motion of the FW and HW is represented as a simple sinusoidal function given by

$$\gamma(t) = -\gamma_m \sin(2\pi ft - \pi/2) \quad (3)$$

where φ_{fm} and φ_{hm} are flapping amplitudes of FW and HW, both of which are equal to 30°. α_m is equal to 30° which represents pitching amplitude. The phase shift between flapping and pitching for both forewing and hindwing keeps at 180°. The flapping frequency f is equal to 30 Hz. The stroke plane angle is equal to 45°, the sweeping amplitude γ_m of FW and HW varies equally to 0°, 5°, 10°, 15°, 20°, 25°, 30° and 35°.

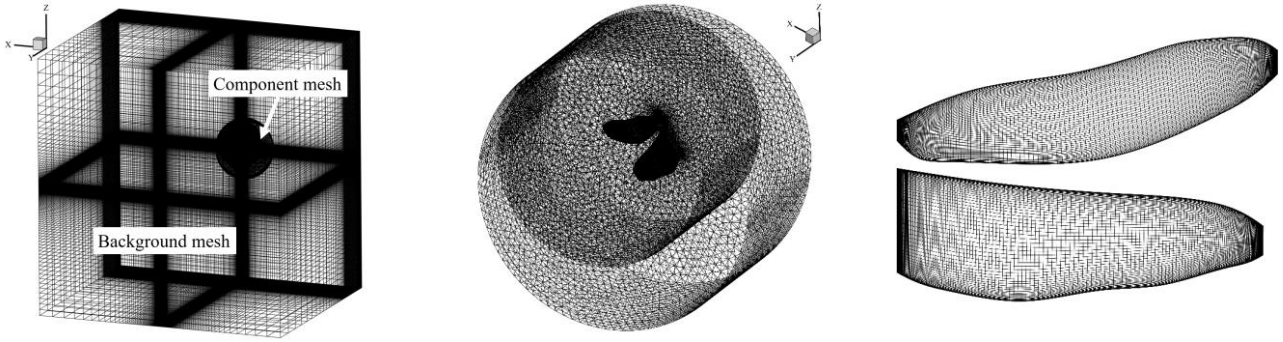

(a) Assembled mesh (b) Component mesh (c) Wing surface mesh

Fig 2 Computational setup for the tandem wing

2.2 Flow solver

The transient simulations are investigated numerically using the computational fluid dynamics software Fluent(Fluent Release 19.2) by solving the three-dimensional Navier-Stroke equations. The motion of the flapping wings were conducted based on an overset mesh technique. The overset mesh, consisting of background mesh and component mesh, is considered to be suitable for the large–scale motion simulation. During the dynamic movement, the background mesh stays stationary, while the entire component mesh moves as a rigid body. The motion of flapping wing is adjusted by modifying a User Defined Function (UDF) in the form of coordinate transformation. While the wing is moving, the mesh around the wing in the deformable zone is updated using dynamic mesh technology. The

Reynolds number is calculated with the velocity at R2. The radius of the second moment of forewing area R2 equals 34.3mm. The Reynolds number is:

$$U_{\text{ref}} = 4f\varphi_m R_2 = 2.2m/s \tag{4}$$

$$\text{Re} = \frac{U_{ref}\text{c}_\text{f}}{\nu} = 1286 \tag{5}$$

where c_f is the mean aerodynamic chord and ν is the kinematics viscosity which equals to the ratio of dynamic viscosity and density. Laminar model is adopted to simulate the low Reynold flow situation. The boundary condition of the outlet is pressure outlet. The boundary type of the component zone is overset. No-silp wall condition is applied to both fore and hind wings. Momentum, turbulent kinematic energy, and specific dissipation rate are discretized with second-order upwind scheme. Second-order accuracy is applied to calculate the pressure. The coupled algorithm is employed for the pressure-velocity coupling. The computational mesh consists of background mesh and component is shown in Fig 2.

2.3 Time step independence validation

Time step size validation was processed for the bionic wing model before CFD analysis. Time step of T/100, T/200 and T/400 are employed for simulation respectively. As showed in Fig 3, the periodic vertical force and the periodic power for three time step sizes have no obvious difference. Therefore, a time step size T/200 is employed for follow-up simulations. We give the formulas for calculating the aerodynamic power first, then the power required to overcome the aerodynamic torque is called the aerodynamic power P, which can be given as follows:

$$P = -\left(\text{M}_x \bullet \dot{\varphi} + M_y \bullet \dot{\alpha} + \text{M}_z \bullet \dot{\gamma}\right) \tag{6}$$

where M_x is the torque around the axis of flapping motion, M_y is the torque around the axis of pitching motion and M_z is the torque around the axis of sweeping motion. $\dot{\varphi}$, $\dot{\alpha}$ and $\dot{\gamma}$ are the first-order derivatives of φ, α and γ versus time, respectively.

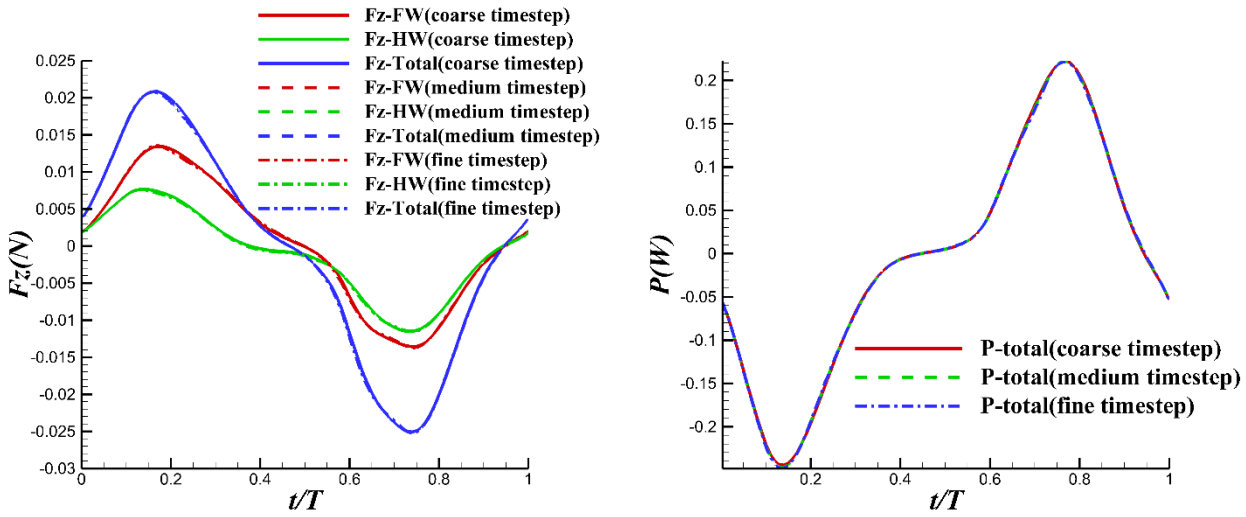

(a) comparison of periodic vertical force (b) comparison of periodic power

Fig 3 Validation of time step size

3. Results and discussion

3.1 Force and power

The results of vertical force, horizontal force and Power of different sweeping amplitudes are shown in Fig 4. From the periodic vertical force of forewing, it can be seen that with the increase of the sweeping amplitude, the magnitude of the peak vertical force first decreases and then increases

during downstroke. The time corresponding to the peak vertical force is continuously delayed. For hindwing, there are two peaks during downstroke. As the sweep amplitude increases, the magnitude of the first peak first increases then decreases while the magnitude of the second peak corresponding to the flapping reversal keeps increasing. By observing the trend of the total vertical force, the increase of the sweeping amplitude can cause the positive lift amplitude to decrease first and then increase. The corresponding time will be delayed. From time-averaged vertical force, the increase of sweeping amplitude in the hovering state can indeed enhance the vertical force as a whole, and the hindwing plays a significant role in enhancing the vertical force.

It can be seen from the periodic horizontal force of the forewing in the downstroke that as the sweeping amplitude increases, the magnitude of the negative peak value keeps going up. For the hindwing periodic horizontal force, the force increases simultaneously with the sweeping amplitude during stroke reversal. From the time-averaged horizontal force, as the sweeping amplitude increases, the time-averaged horizontal force of the forewing continues to increase, while the time-averaged horizontal force of hindwing first decreases, and then gradually increases after the sweeping amplitude is equal to 10°. From the point of view of the force, the sweeping amplitude has little effect on the vertical force and the horizontal force.

For the periodic output power of the forewing, it can be found that the sweeping amplitude will have an impact on the output power, especially in the downstroke. In the downstroke, as the sweeping amplitude increases, the valley value of output power in the first half of the cycle also increases, while the output power changes slightly in the remaining half cycle. For the hindwing, the decrease of output power is accompanied by the increase of sweeping amplitude during stroke reversal. More importantly, it can be found from the time-averaged power of forewing and total wings that as the sweeping amplitude increases, the output power continues to go up, which consumes more energy for dragonfly. And for the hindwing, as the sweeping amplitude increase, the time-averaged output power first decrease and then increase gradually.

Results of force and power consumption show that for the hovering dragonflies, the sweeping motion increases the vertical force slightly, but the power consumption increases severely compared with the vertical force. As the sweeping amplitude of forewings and hindwings increases from 0° to 35° equally, the time-averaged vertical force increases by about 3.23×10^{-3}g , while the power consumption increases by about $0.0256W$. From the time-averaged vertical and horizontal forces, it can be concluded that although the forewings and hindwings have the same motion law, their variation trends are not the same, which indicates that the forewings interfere with the hindwings for tandem wings distribution.

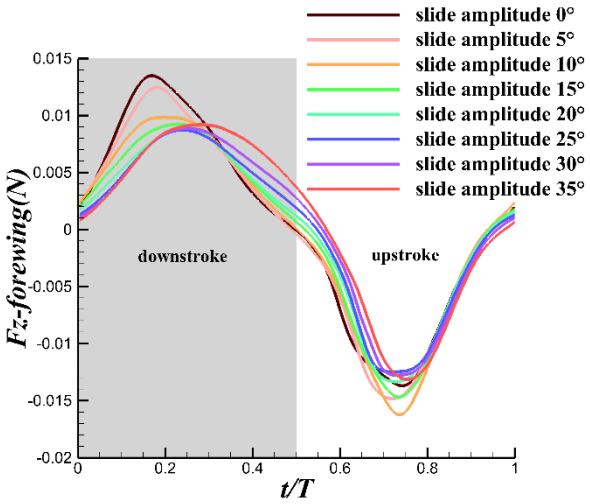

(a)Periodic vertical force of forewing

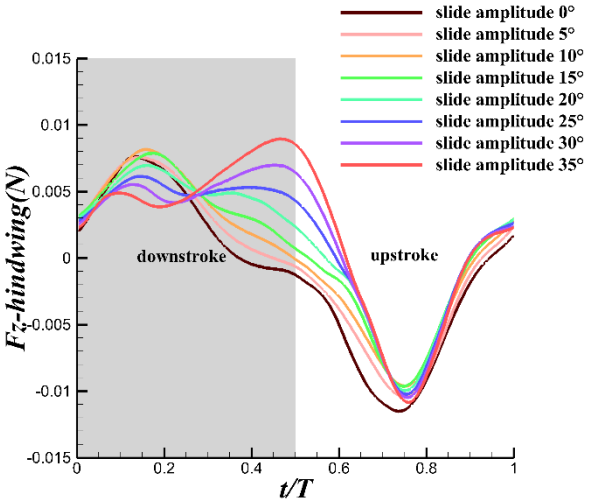

(b)Periodic vertical force of hindwing

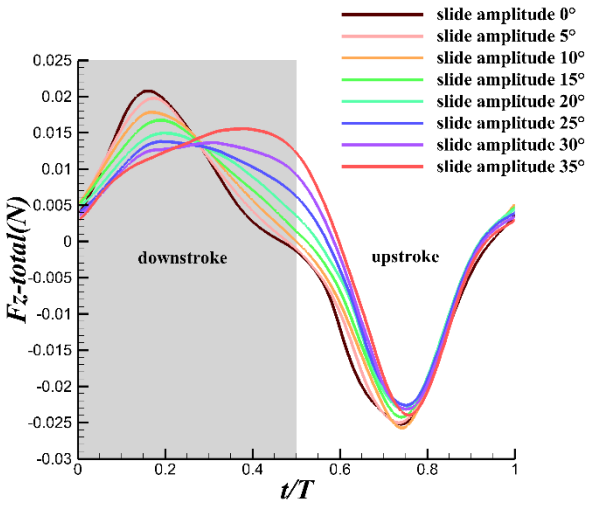

(c)Periodic vertical force of total wings

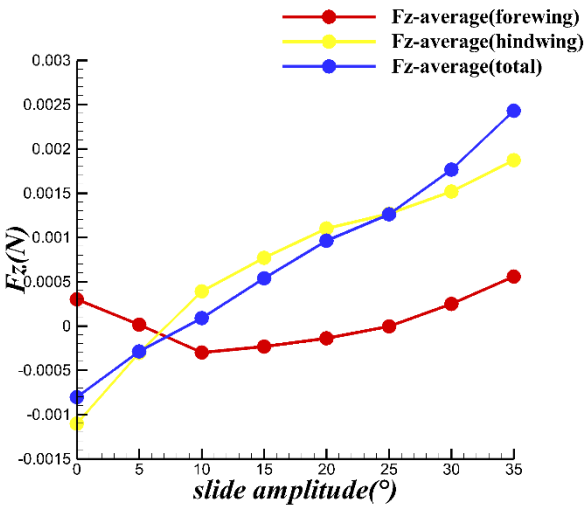

(d)Time-averaged vertical force

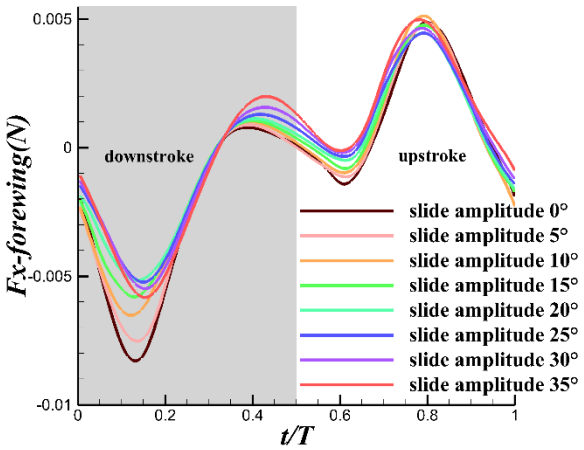

(e)Periodic horizontal force of forewing

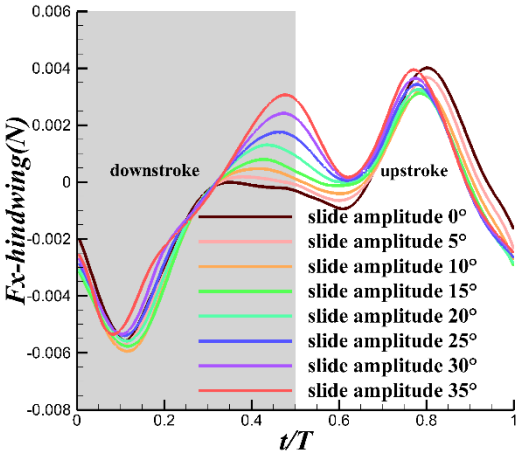

(f)Periodic horizontal force of hindwing

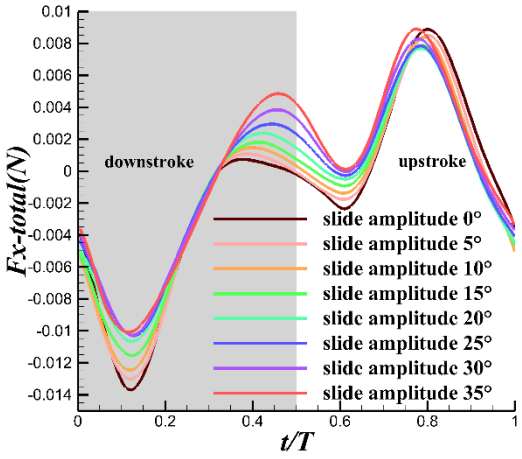

(g)Periodic horizontal force of total wings

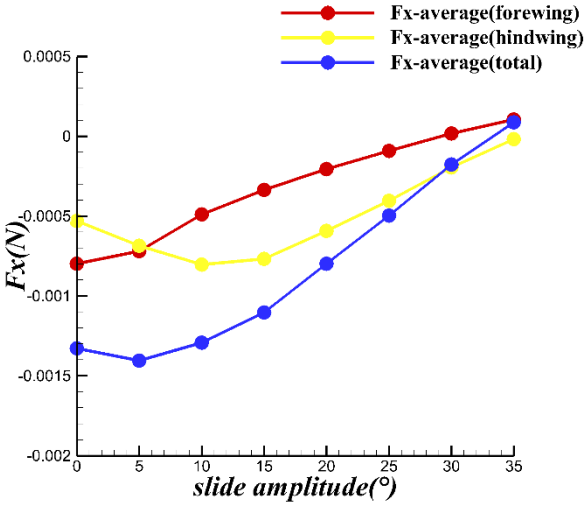

(h)Time-averaged horizontal force

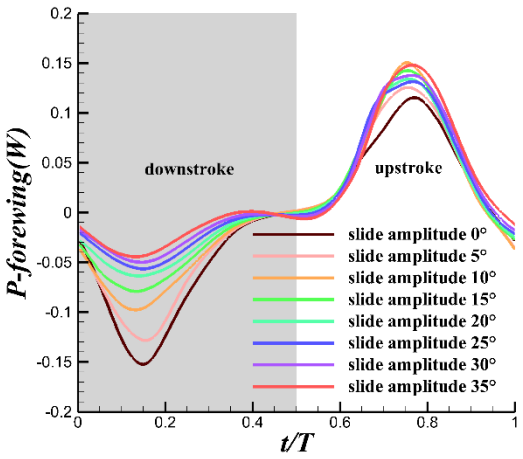

(i)Periodic power of forewing

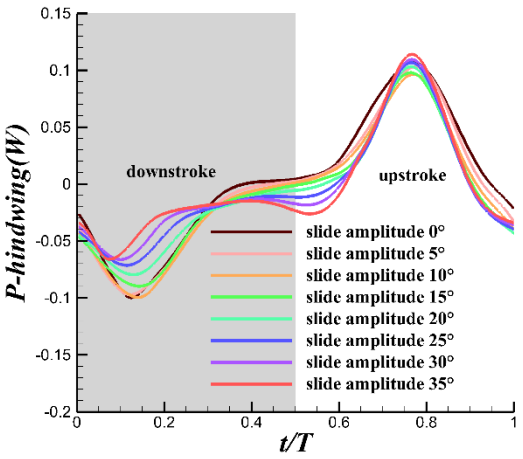

(j)Periodic power of hindwing

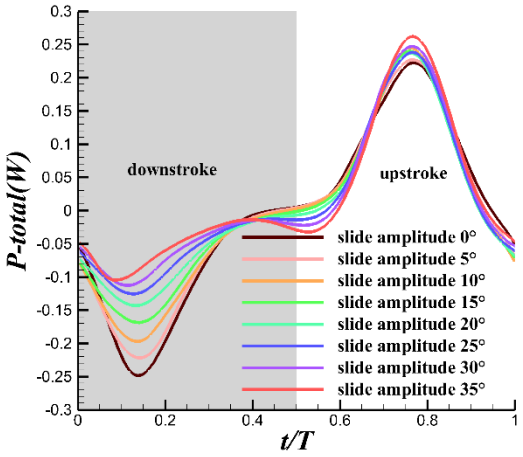

(k)Periodic power of total wings

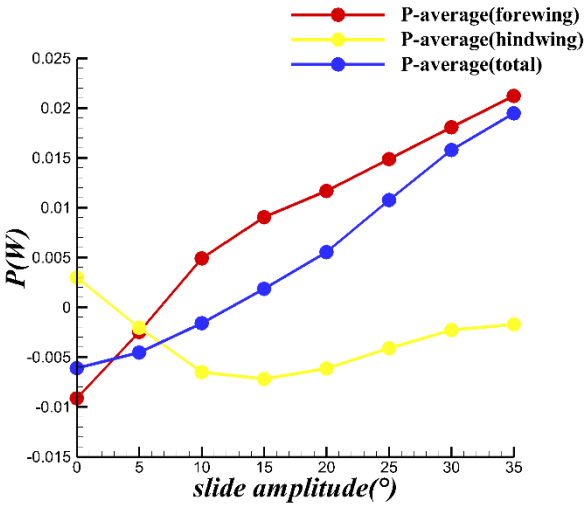

(l)Time-averaged power

Fig 4 Force and Power result of different sweeping amplitude

3.2 Flow structures

To understand the underlying flow phenomena that results in force modulation on the tandem wings, we have visualized the flow at critical time instants: t/T=0, 0.125, 0.5 and 0.75. In Fig 5, the flow features at the beginning of the downstroke and upstroke (t/T=0 and t/T=0.5), around middle of the upstroke (t/T=0.75) and around the time corresponding to the positive peak value in the downstroke (t/T=0.125). The flow structures are colored according to the pressure values.

Fig 5 shows the iso-surfaces of Q criterion is equal to 400000. At t=0.125T, it is obvious that the low pressure area on the forewing decreases with the increase of sweeping amplitude which leads to more power consumption. It can be clearly observed that the sweeping motion delays a development of the vortices during stroke reversal (t/T=0.5). With the increase of the sweeping amplitude, the trailing edge vortex shedding becomes slower, which makes the low-pressure area of the hindwing larger, thus reflecting the increase of the vertical force during stroke reversal. During stroke reversal, obvious leading edge vortices can be observed. The radius of the leading edge vortices from the wing heel to the wing tip becomes larger and larger and the vortices gradually falls off.

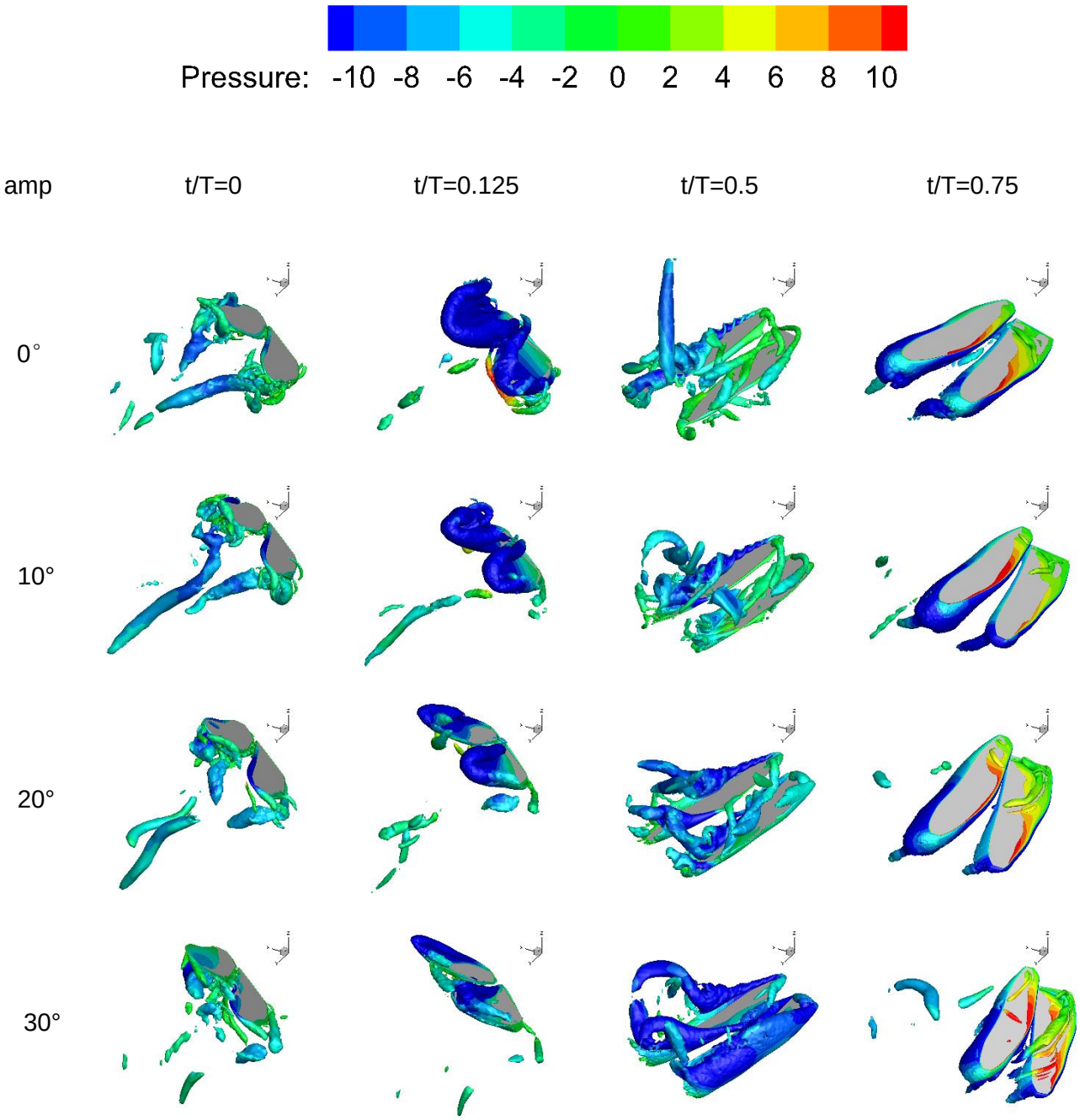

Fig 5 Iso-Surfaces of Q-criterion

From the spanwise slice of y vorticity in Fig 6, it can be observed that the trailing edge vortices on the hindwings delay shedding with the increase of sweeping amplitude during stroke reversal. The vorticity on the upper surface of the wings in the middle of the downstroke decreases as the increase of the sweeping amplitude. The vorticity from heel to tip of the wing increases gradually and tends to fall off.

In order to simply explore the influence of sweeping motion, the motion law of the forewings and the hindwings is the same in this paper. The wake capture of the hindwings over the forewings could not be observed. However, we can still find that the trailing edge vortices shedding from the forewings will have an impact on the hindwings during stroke reversal.

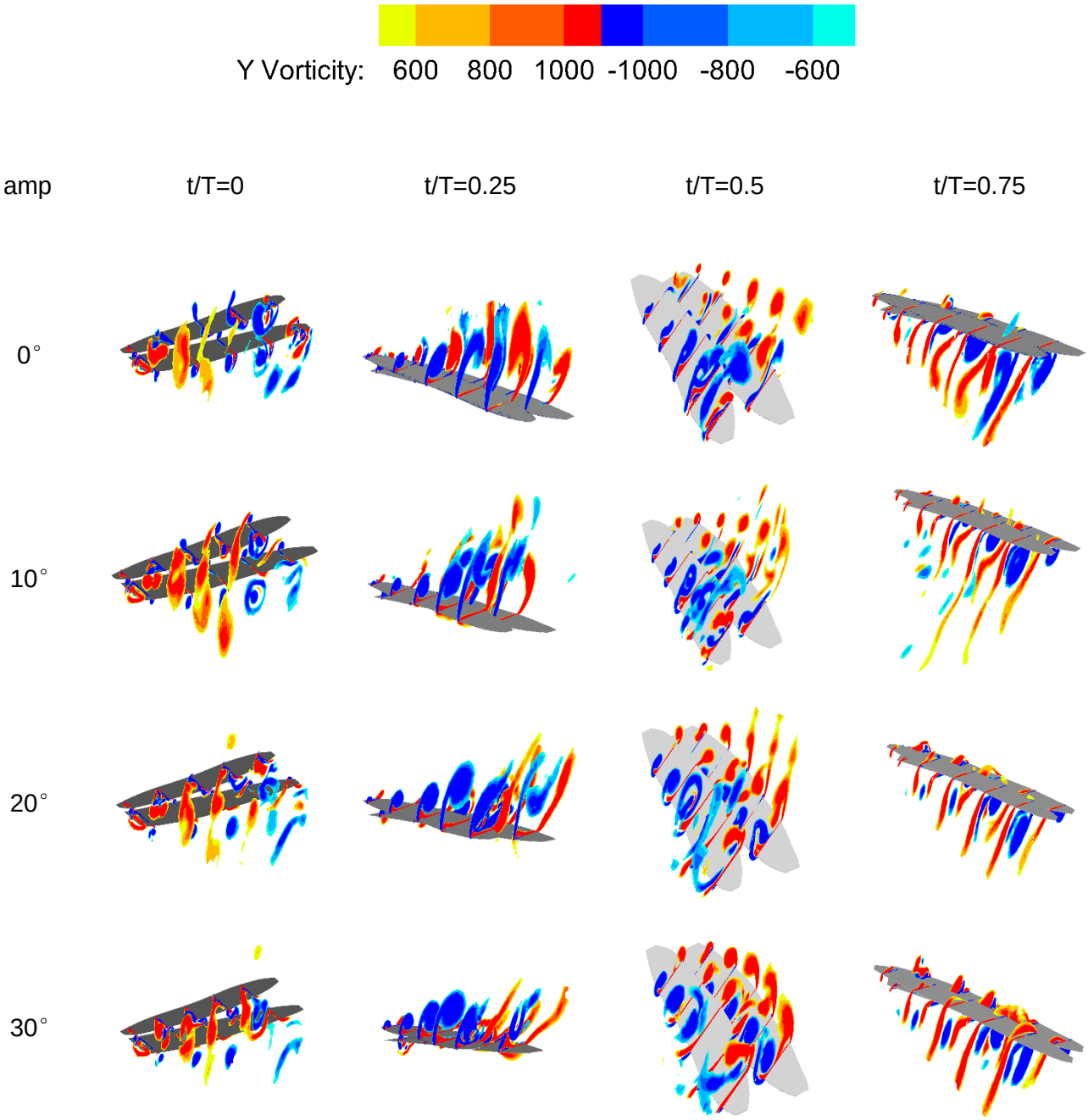

Fig 6 Spanwise slice of y vorticity

4. Conclusions

A transient numerical method based on the overset mesh technique is used to investigate parametric influences, notably the sweeping amplitude during the flapping cycle. The shape of simulated wing is similar to that of a real dragonfly.

It can be concluded that the sweeping motion increases the vertical force slightly, but the power consumption increases severely compared with the vertical force. As the sweeping amplitude of forewings and hindwings increases from 0° to 35° equally, the time-averaged vertical force increases by about 3.23×10^{-3}g , while the power consumption increases by about $0.0256W$. For the forewings, the change of the sweeping amplitude mainly affects the peak value of the vertical force and the corresponding time of the peak in the downstroke. The difference of vertical force on the

hindwings is mainly occurs during the stroke reversal. The hindwing plays a more significant role than forewing in enhancing the vertical force. In terms of the horizontal force, the change caused by the increase of the sweeping amplitude mainly occurs at the peak in the downstroke of the forewings and the stroke reversal of the hindwings.

From the perspective of the flow structure, the sweeping motion, especially the increase in sweeping amplitude, will delay the shedding of the trailing edge vortices. From the heel to the tip, the leading edge vortices gradually increase in radius and fall off. The vortices shedding from the forewings will have a certain impact on the hindwings of tandem distribution.

The sweeping motion may not improve the aerodynamic performance of tandem wings in hovering state, but it may be helpful for forward flight or climbing. Our research can provide reference for the design of dragonfly-like aircraft with multi degree of freedom motion.

5. Contact Author Email Address

Mailto:zhuzc980407@163.com

6. Copyright Statement

7. Acknowledgments

This study was supported by the National Natural Science Foundation of China (11872314) and the Key R&D Program in Shaanxi Province of China (2020GY-154).

References

[1] Dickinson, M. H. and Götz, H.G. (1993). Unsteady aerodynamic performance of model wings at low Reynolds numbers. J. Exp. Biol. 174, 45–64.

[2] Wakeling J M, Ellington C P. Dragonfly flight. II. Velocities, accelerations and kinematics of flapping flight. Journal of experimental biology, 1997, 200(3): 557-582.

[3] Sane S. P. (2003). The aerodynamics of insect flight. J. Exp. Biol. 206, 4191–4208.

[4] Thomas A L R, Taylor G K, Srygley R B, et al. Dragonfly flight: free-flight and tethered flow visualizations reveal a diverse array of unsteady lift-generating mechanisms, controlled primarily via angle of attack[J]. Journal of Experimental Biology, 2004, 207(24): 4299-4323.

[5] Tsuyuki K, Sudo S, Tani J. Morphology of insect wings and airflow produced by flapping insects[J]. Journal of intelligent material systems and structures, 2006, 17(8-9): 743-751.

[6] Broering, M. T., Lian, Y. S. and Henshaw, W. (2012). Numerical investigation of energy extraction in a tandem flapping wing configuration. AIAA J. 50, 2295-2307

[7] Chen Y H, Skote M, Zhao Y, et al. Dragonfly (Sympetrum flaveolum) flight: Kinematic measurement and modelling[J]. Journal of Fluids and Structures, 2013, 40: 115-126.

[8] Kok, J. M., Gih Keong Lau, and J. S. Chahl. On the aerodynamic efficiency of insect-inspired micro aircraft employing asymmetrical flapping[J]. Journal of Aircraft 2016, 53(3): 800-810.

[9] Bomphrey R J, Nakata T, Henningsson P, et al. Flight of the dragonflies and damselflies[J]. Philosophical Transactions of the Royal Society B: Biological Sciences, 2016, 371(1704): 20150389.

[10] Li C, Dong H. Wing kinematics measurement and aerodynamics of a dragonfly in turning flight[J]. Bioinspiration & Biomimetics, 2017, 12(2): 026001.

[11] Luo G, Du G, Sun M. Effects of Stroke Deviation on Aerodynamic Force Production of a Flapping Wing[J]. AIAA Journal, 2018, 56(1):25-35.

[12] Hefler C, Qiu H, Shyy W. Aerodynamic characteristics along the wing span of a dragonfly Pantala Flavescens[J]. Journal of Experimental Biology, 2018, 221(19): jeb171199.

[13] Shanmugam A R, Sohn C H. Numerical investigation of the aerodynamic benefits of wing-wing interactions in a dragonfly-like flapping wing[J]. Journal of Mechanical Science and Technology, 2019, 33(6): 2725-2735.

[14]Zou P Y, Lai Y H, Yang J T. Effects of phase lag on the hovering flight of damselfly and dragonfly. Physical Review E, 2019, 100(6): 063102.

[15]Nagai H, Fujita K, Murozono M. Experimental Study on Forewing–Hindwing Phasing in Hovering and Forward Flapping Flight[J]. AIAA journal, 2019, 57(9): 3779-3790.

[16]Lehmann F O, Wehmann H N. Aerodynamic interference depends on stroke plane spacing and wing aspect ratio in damselfly model wings[J]. International Journal of Odonatology, 2020, 23(1): 51-61.

[17]Arranz G, Flores O, García-Villalba M. Three-dimensional effects on the aerodynamic performance of flapping wings in tandem configuration[J]. Journal of Fluids and Structures, 2020, 94: 102893.